Biochemical and Biophysical Research Communications 430 (2013) 1206–1211

Contents lists available at SciVerse ScienceDirect

Biochemical and Biophysical Research Communications

journal homepage: www.elsevier.com/locate/ybbrc

Structural analysis of an epsilon-class glutathione transferase from housefly, *Musca domestica*

Chihiro Nakamura [a], Shunsuke Yajima [b], Toru Miyamoto [a], Masayuki Sue [a,*]

[a] Department of Applied Biology and Chemistry, Tokyo University of Agriculture, Sakuragaoka 1-1-1, Setagaya, Tokyo 156-8502, Japan
[b] Department of Bioscience, Tokyo University of Agriculture, Sakuragaoka 1-1-1, Setagaya, Tokyo 156-8502, Japan

ARTICLE INFO

Article history:
Received 28 November 2012
Available online 22 December 2012

Keywords:
Crystal structure
Epsilon class
Glutathione transferase
Musca domestica

ABSTRACT

Glutathione transferases (GSTs) play an important role in the detoxification of insecticides, and as such, they are a key contributor to enhanced resistance to insecticides. In the housefly (*Musca domestica*), two epsilon-class GSTs (MdGST6A and MdGST6B) that share high sequence homology have been identified, which are believed to be involved in resistance against insecticides. The structural determinants controlling the substrate specificity and enzyme activity of MdGST6s are unknown. The aim of this study was to crystallize and perform structural analysis of the GST isozyme, MdGST6B. The crystal structure of MdGST6B complexed with reduced glutathione (GSH) was determined at a resolution of 1.8 Å. MdGST6B was found to have a typical GST folding comprised of N-terminal and C-terminal domains. Arg113 and Phe121 on helix 4 were shown to protrude into the substrate binding pocket, and as a result, the entrance of the substrate binding pocket was narrower compared to delta- and epsilon-class GSTs from Africa malaria vector *Anopheles gambiae*, agGSTd1-6 and agGSTe2, respectively. This substrate pocket narrowing is partly due to the presence of a π-helix in the middle of helix 4. Among the six residues that donate hydrogen bonds to GSH, only Arg113 was located in the C-terminal domain. Ala substitution of Arg113 did not have a significant effect on enzyme activity, suggesting that the Arg113 hydrogen bond does not play a crucial role in catalysis. On the other hand, mutation at Phe108, located just below Arg113 in the binding pocket, reduced the affinity and catalytic activity to both GSH and the electrophilic co-substrate, 1-chloro-2,4-dinitrobenzene.

1. Introduction

Cytosolic glutathione transferases (GSTs) comprise a large multifunctional enzyme family found in a wide variety of organisms from microbes to higher animals. One of the major biological roles for GSTs is to catalyze the conjugation of electrophilic xenobiotics to glutathione (GSH), which increases their water solubility and allows them to be more easily excreted [1]. In insects, some members of the GST family are believed to be involved in resistance against insecticides [2].

In the housefly (*Musca domestica*), GSTs have been divided into two immunologically distinct classes, class I and class II. As sequence data of GSTs from various insects including *Drosophila melanogaster*, *Anopheles gambiae*, and *Anopheles dirus* have been compiled, it has become difficult to assign some GSTs to either class I or class II. Therefore, the nomenclature system of mammalian GSTs was adopted for insect enzymes, in which GSTs are classified based on their amino acid sequences. Among the classified enzymes, delta and epsilon classes are unique to insects [3,4].

MdGST1, a member of the delta GST class that was cloned for the first time from the housefly, has been suggested to contribute to elevated resistance against insecticides [1,2]. Other isozymes of the delta-class GST, MdGST2–MdGST4, were cloned and characterized by Syvanen et al. [5], and MdGST3 was proposed as a candidate GST that endows the housefly with insecticide resistance [5,6]. Furthermore, Wei et al. [7] demonstrated that additional housefly isozymes (MdGST6A and MdGST6B) belonging to the epsilon class function as key enzymes in the detoxification of insecticides such as methyl parathion and lindane. It was suggested that the detoxification capability of housefly GST against insecticides is correlated to its catalytic activity with 1,2-dichloro-4-nitrobenzene (DCNB) rather than 1-chloro-2,4-dinitrobenzene (CDNB) [8]. CDNB is known to serve as a good substrate for both delta and epsilon GSTs from the housefly, but DCNB is effectively accepted only by the epsilon GST class [7]. Therefore, elucidation of the structural basis for different substrate recognition by housefly delta and epsilon GSTs would greatly contribute to our understanding of the molecular mechanisms involved in insecticide resistance. While there have been some reports of crystal structure analyses of delta- and epsilon-class GSTs from a variety of insects, no crystal structures of housefly GSTs have been

* Corresponding author. Fax: +81 3 5477 2323.
E-mail address: sue@nodai.ac.jp (M. Sue).

0006-291X/$ - see front matter © 2013 Elsevier Inc. All rights reserved.
http://dx.doi.org/10.1016/j.bbrc.2012.12.077

disclosed. In this study, crystallization and structural analysis of MdGST6B was performed, and the epsilon class GST was demonstrated to have high activity toward DCNB as well as CDNB.

2. Materials and methods

2.1. Cloning and expression of MdGST6B

MdGST6B (GenBank accession No., AF147206) was cloned by RT-PCR using total RNA as a template prepared from the abdomens of an organophosphorous insecticide-resistant housefly strain, Yachiyo, that was maintained in our laboratory. MdGST6B cDNA was obtained by reverse transcription using Superscript III (Invitrogen) with an oligo (dT) primer followed by PCR using Taq DNA polymerase (QIAGEN) with gene specific primers. The amplified DNA was ligated into the *Nde*I-*Hin*dIII site of pET21a and pET28a (Novagen) to obtain the enzyme with and without an N-terminal His-tag, respectively. The resulting plasmids were then transferred into *Escherichia coli*, BL21 CodonPlus(DE3)-RIL (Stratagene). Expression of GST was performed by adding isopropyl-β-D-thiogalactopyranoside at a concentration of 1 mM followed by overnight incubation at 20 °C with vigorous aeration. The cells were pelleted by centrifugation (3500*g* for 5 min) and then re-suspended in 5 mL of a solution of 10 mM Na_2HPO_4, 1.8 mM KH_2PO_4, 140 mM NaCl, and 2.7 mM KCl (pH 7.3). The cells were disrupted by sonication on ice (several 20-s pulses at a power setting of 100 W). The soluble protein fraction was recovered by collecting the supernatant after centrifugation at 15,000*g* for 10 min. The wild type GST was loaded onto a GSTrap FF column (GE Healthcare) equilibrated in 10 mM Tris–HCl, pH 7.4, and after washing non-specifically bound proteins with the same buffer, GST was eluted with 50 mM Tris–HCl, pH 8.0, containing 10 mM of reduced glutathione (GSH). The N-terminal His-tagged protein was purified by metal chelation chromatography. The soluble fraction was applied to a HisTrap HP column (GE Healthcare) charged with Ni^{2+} and equilibrated in 20 mM phosphate buffer, pH 7.4, containing 0.5 M NaCl and 10 mM imidazole. After washing the column with the same buffer containing 0.5 M NaCl and 60 mM imidazole, the GST was eluted by increasing the concentration of imidazole to 300 mM.

2.2. Site-directed mutagenesis

GST mutants were generated by an inverse-PCR based method using MdGST6B genes in pET28a (mentioned above) as templates. The primer sets used for PCR were as follows: F108G, 5′-ggtcagggaggtttacgcaacatta (forward) and 5′-taagacaccagcttcgaagtacatg (reverse); R113A, 5′-aacattaccgcccc-cattgttcttt (forward) and 5′-ggctaaacctccctgaaataagac (reverse). The reaction was carried out using PrimeStar Max DNA polymerase (Takara Bio) with denaturing at 98 °C and annealing and polymerization at 68 °C. The resulting blunt-end DNA fragment was purified by agarose-gel electrophoresis followed by phosphorylation and self-ligation using the BKL Kit (Takara Bio). The product was then transferred into DH5α. After sequence verification, the plasmid was introduced into BL21 CodonPlus (DE3)-RIL.

2.3. Enzyme assay

The enzyme activity of GST was measured spectrophotometrically according to the method of Habig et al. [9]. The kinetic parameters for CDNB were determined by varying its concentration with a constant GSH concentration of 1 mM, and the parameters for GSH were determined by changing the GSH concentration with a constant CDNB concentration of 0.5 mM. The data were fit to the Michaelis–Menten equation using SimaPlot (SPSS).

2.4. Crystallization and structure determination

For crystallization, 10 mg/ml of the purified MdGST6B (without the N-His-tag) in 10 mM Tris–HCl (pH 8.0) and 10 mM GSH were mixed in a 1:1 ratio with a reservoir solution containing 0.1 M HEPES-NaOH, pH 7.0, and 1.2 M Na citrate. Crystals were prepared by the hanging drop vapor diffusion method at 20 °C, that grew to dimensions of 0.3 × 0.2 × 0.2 mm in a couple of days.

Diffraction data for MdGST6B were collected with beamline 5A, at the Photon Factory. The crystals were quick-soaked in a mixture of the reservoir solution and 7 M sodium formate in a 1:1 ratio and flash frozen in a cold stream of nitrogen gas at 100 K. The datasets were merged and processed with the programs MOSFLM [10] and SCALA [11], respectively, in the CCP4 suite [12]. The initial structure of MdGST6B was solved by molecular replacement using the program MOLREP [13] in the CCP4 suite using the coordinates of mosquito glutathione transferase (PDB code: 1JLV) as a target model. Refinements for both structures were carried out first with the program CNS [14] without using NCS because the electron density was well defined, and thereafter, with the program REFMAC5 [15] in the CCP4 suite.

3. Results and discussion

3.1. The overall structure of MdGST6B

The structure of MdGST6B (without an N-terminal His-tag) was refined at 1.8 R/R_{free}-factors of 17.8/20.6%. Detailed statistics for the data collection and refinement are given in Table 1. The atomic coordinates of TaGlu1b were deposited in the Protein Data Bank under the code 3VWX. The structure of the functional dimer of MdGST6B is shown in Fig. 1A and its subunit is shown in Fig. 1B. MdGST6B adopted the canonical GST fold with two domains connected by a short linker segment (residues 80–89). The N-terminal domain (residues 1–79) consisted of four β-strands and three

Table 1
Data collection and refinement statistics.

	GST6B
PDB ID	3VWX
Data collection	
Beamline	PF-5A
Wavelength (Å)	1.0000
Space group	$P3_1$
Cell unit (Å, °)	$a = b = 87.55$, $c = 131.88$
Number of subunits per ASU	4
Resolution range (Å)	75.81–1.80 (1.90–1.80)
Completeness (%)	98.3 (97.4)
I/σ (I)	7.5 (2.0)
Redundancy	5.5 (5.4)
R_{merge}[a]	0.065 (0.372)
Number of unique reflections	102983 (14869)
Refinement	
Resolution (Å)	65.82–1.80 (1.847 – 1.8)
Number of reflections	97850 (7102)
R/R_{free}[b]	0.164/0.191 (0.229/0.277)
Number of atoms	
Protein	6924
Solvent	948
RMSD from ideality	
Bond length (Å)	0.014
Bond angle (°)	1.370
Average B factor (Å2)	
Protein	25.76
Solvent	36.88

The numbers in parentheses are given for the highest resolution shells.
[a] $R_{merge} = \Sigma h \Sigma i |I_i(h) - < I(h) > | \Sigma h \Sigma i I_i(h)$, where $I_i(h)$ is the ith measurement.
[b] A subset of the data (5%) was excluded from the refinement and was used to calculate R_{free}.

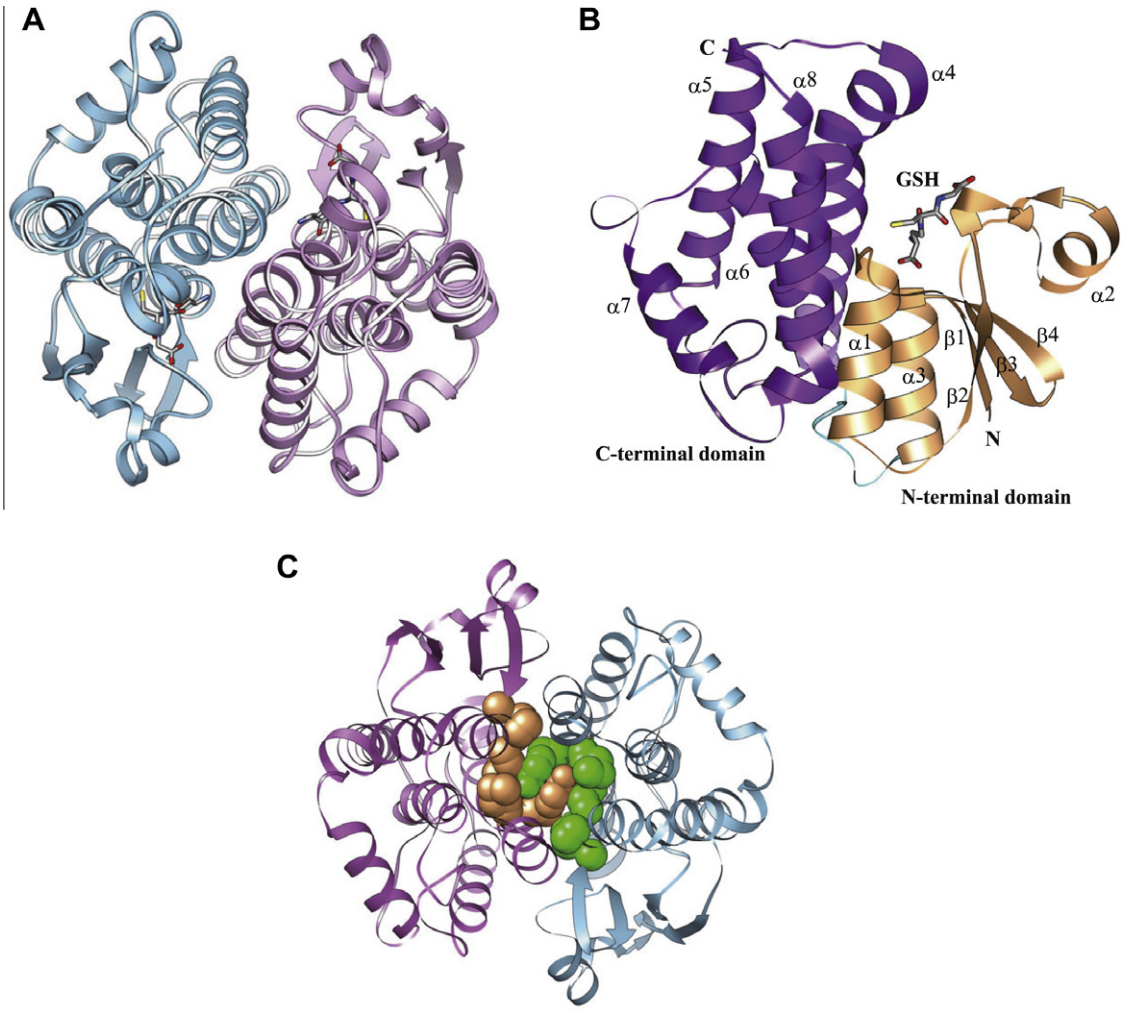

Fig. 1. Tertiary structure of MdGST6B. (A) a ribbon diagram representation of the functional MdGST6B dimer. Each subunit is depicted in cyan or pink. (B) a ribbon diagram representation of the MdGST6B monomer. The N-terminal and C-terminal domains are drawn in light orange and purple, respectively, and the linker region is drawn in cyan. (C) the lock and key structure at the subunit interface. Residues participating in the lock and key motif are represented in a sphere. Note that the structure is drawn from the point of view opposite to A. In A and B, GSH is shown in a stick model with nitrogen, oxygen, and sulfur atoms indicated in blue, red, and yellow, respectively. (For interpretation of color in Fig. 1, 2 and 4, the reader is referred to the web version of this article.)

α-helices: the central four β-strands were flanked on one side by two α-helices and on the other side by one helix. This domain was arranged in the βαβαββα motif, and the mixed β-sheet adopted a $-1+2+1$ topology. The C-terminal domain was comprised of a right-handed bundle of four α-helices. Helix 4 was slightly bent in the middle, similar to the other known GSTs. At the subunit interface, the lock-and-key motif that is required for stabilization of the dimer was observed (Fig. 1C). This motif is common for various classes of GST [16]. The residues Asn67, His69, and Tyr101 in the MdGST6B monomer function as a 'key', and the residues Ala70, Met100, Tyr101, and Ala104 in the other subunit function as a 'lock'.

For *A. gambiae*, 12 delta-class and 8 epsilon-class GST genes have been identified [17]. Crystals of GSTs from the both classes have been obtained and their structures have been compared with each other [18,19]. MdGST6B shares 45% amino acid-sequence identity with agGSTe2, an epsilon-class GST from *A. gambiae* that possesses high detoxification activity toward DDT, and 38% identity with agGSTd1-6, a delta-class GST from *A. gambiae* whose contribution to DDT detoxification is considered to be much smaller than agGSTe2. In Fig. 2A, the structure of MdGST6B was superimposed onto those of agGSTe2 and agGST1-6 to compare their structures. The backbones of the N-terminal domains are almost identical although there is a slight difference in helix 2. On the other hand, the structures of the C-terminal domains seem to be more diverse, especially in helix 4 and helix 8. Disparities in helix 4 and helix 8 were prominent in the latter halves of both helices (upper sides of helix 4 and helix 8 in Fig. 1B and Fig. 2A) that contain substrate binding pockets. Furthermore, helix 8 of the two epsilon-class GSTs (MdGST6B and agGSTe2) protruded into the entrance of the substrate binding pockets compared to that of the delta-class GST. When the amino acid sequences were aligned, the epsilon-class GSTs had longer C-terminal ends than the delta-class GST (Fig. 3). The C-terminal regions of both epsilon GSTs did not have a clear secondary structure and extended outward toward solvent (Fig. 2A). The significance of this region is still unclear.

3.2. The structure around the substrate binding site and effects of site-directed mutagenesis

In the structure of MdGST6B, the mode of GSH binding at the substrate binding site was clearly defined. Direct hydrogen bonds between GSH and the enzyme through Ser12, His53, Val55, Asp67, Ser68, and Arg113 were detected (Fig. 4A). Among these six residues, only Arg113 resided in the C-terminal domain

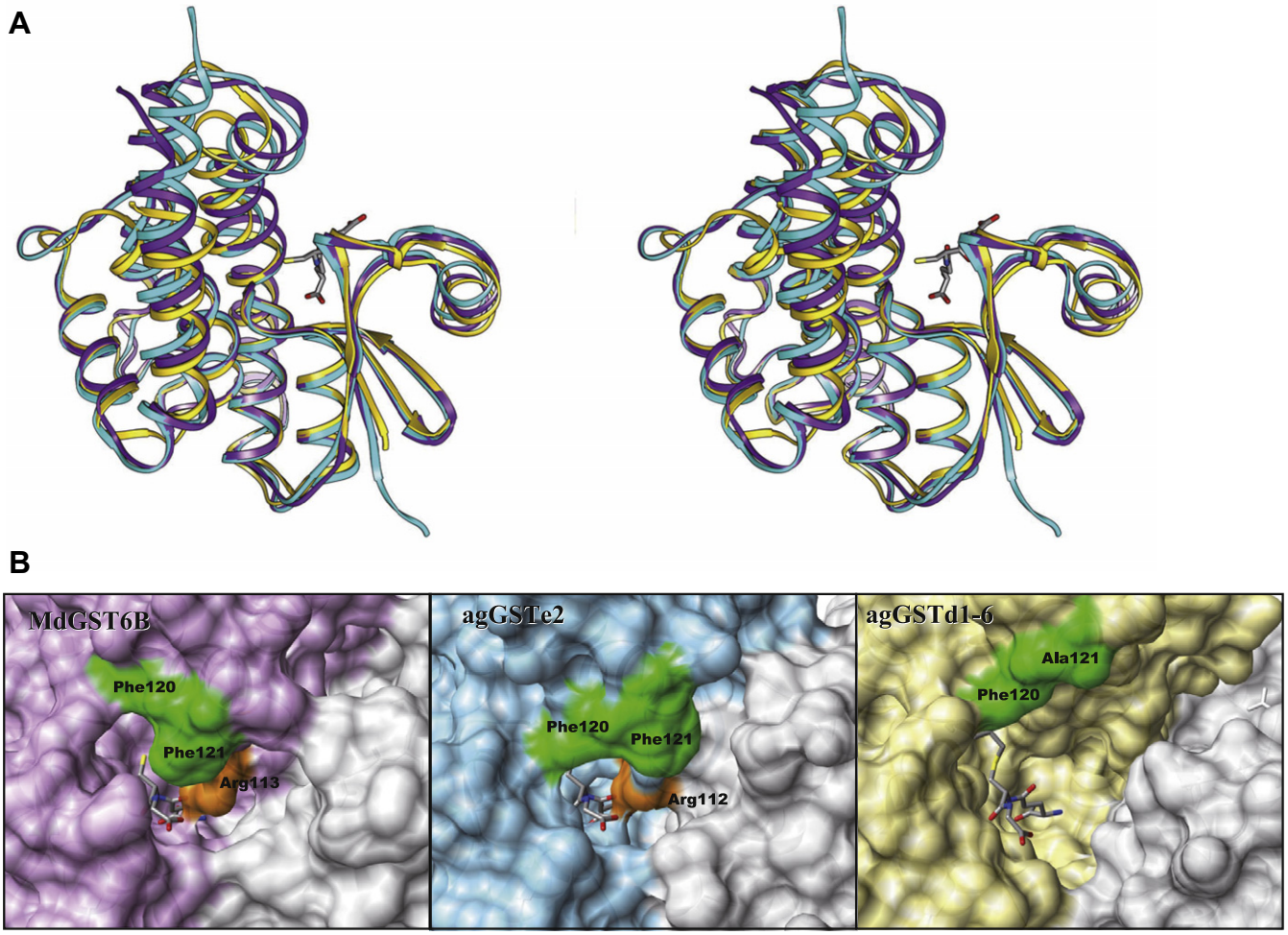

Fig. 2. Comparison of the structures of MdGST6B with epsilon- and delta-class mosquito GSTs. (A) a stereo view of MdGST6B (purple), agGSTe2 (cyan; PDB ID, 2IMI), and agGSTd1-6 (yellow; PDB ID, 1PN9). (B) close up views of the substrate binding pockets. Phe120 and Phe121 in MdGST6B and the corresponding residues in agGSTe2a and agGSTd1-6 are shown in green. Arg113 and Arg112 in MdGST6B and agGSTe2, respectively, are shown in orange. Another subunit is drawn in light gray in each panel. GSH is shown as a stick model.

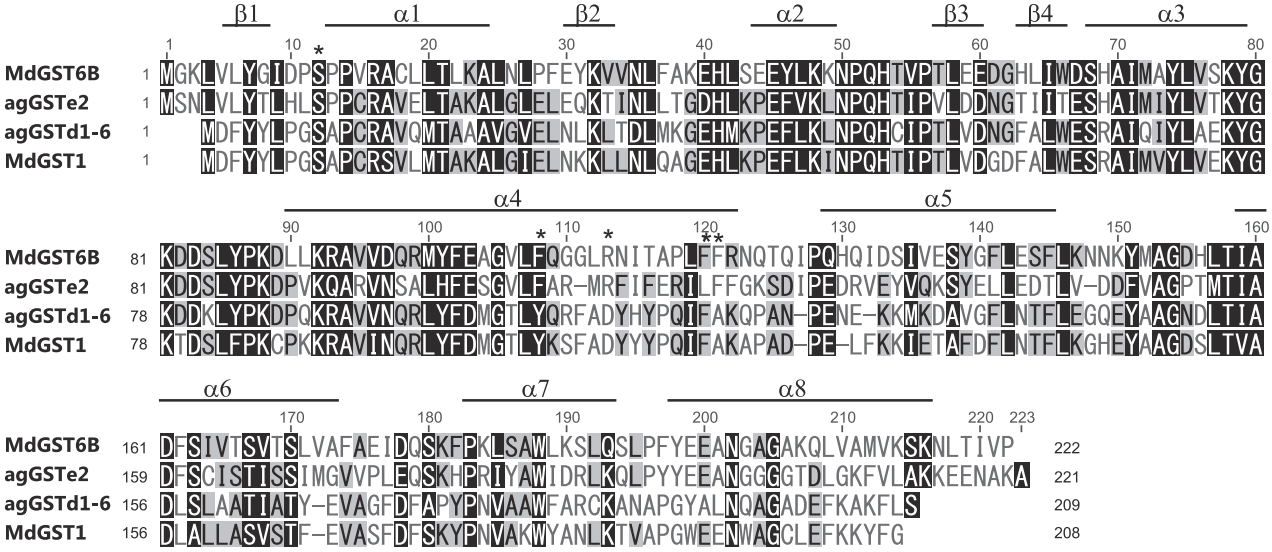

Fig. 3. Sequence alignments of epsilon- and delta-class GSTs from *M. domestica* and *A. gambiae*. The MdGST6B sequence is data obtained in the present study. The Ala at position 70 is replaced by Pro in the sequence in the database (accession number: AF147206). The accession number of MdGST1 is X61302. The sequences of the two mosquito GSTs are based on the sequences deposited in the PDB database. The secondary structures of MdGST6B are indicated above the alignment: Ser12 (catalytic center), Phe108, Arg113, Phe120, and Phe121 of MdGST6B are indicated by asterisks.

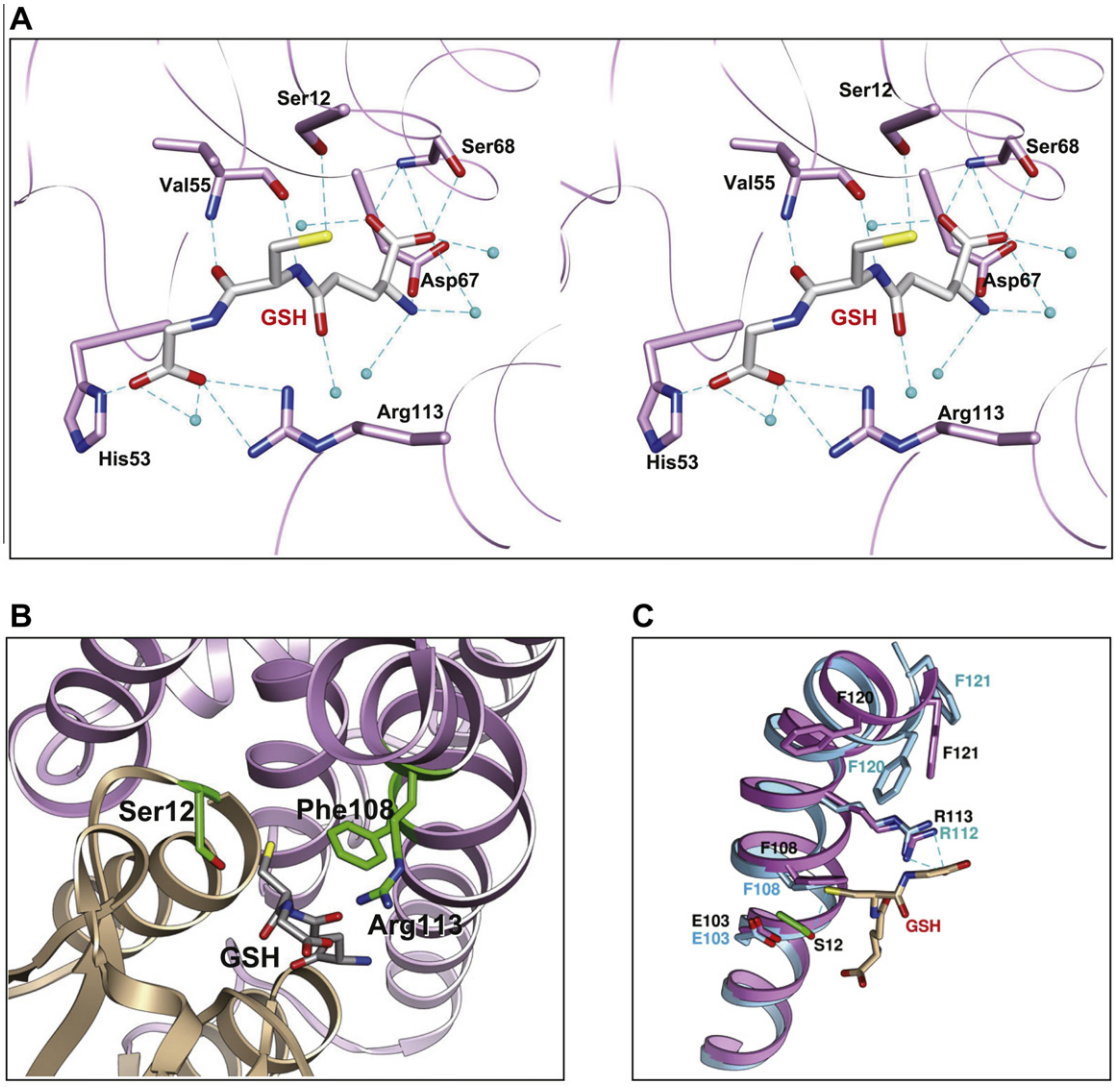

Fig. 4. Architecture of the substrate binding site. (A) a stereo view of the GSH binding site of MdGST6B. Residues forming hydrogen bonds with GSH are shown. Nitrogen, oxygen, and sulfur atoms are depicted in blue, red, and yellow, respectively. Hydrogen bonds are drawn as dashed lines. (B) the interface of the N-terminal and C-terminal domains of the MdGST6B monomer. The side chains of Ser12 (catalytic center), Phe108, and Arg113 are shown as stick models. C, regional structures of helices 4 of MdGST6B (pink) and agGSTe2 (cyan). Note that the backbone amino groups of Arg113 and Phe108 donate hydrogen bonds to the backbone carbonyl groups of Phe108 and Glu103, respectively.

(Fig. 3), which is similar to the case of the mosquito epsilon-class GST, agGSTe2 [18]. Ser12 is known to be highly conserved among delta and epsilon GSTs and to have a role in activating the thiol group of GSH [20]. The oxygen atom in the side chain of Ser12 was located at a distance of 3.06 Å from the sulfur atom of GSH. Furthermore, substitution of this residue with Ala resulted in a loss of enzymatic activity (data not shown), indicating that this residue functions at the catalytic center of the enzyme.

The entrance to the substrate binding pockets of the epsilon GSTs from housefly and mosquito (MdGST6B and agGSTe2, respectively) were narrower than that of the delta-class GST from mosquito, agGSTd1-6 (Fig. 2B). Narrowing of the substrate entrance was mainly effected by residues Arg113, Phe120, and Phe121 of the epsilon GSTs. In MdGST6B, the side chain of Phe121 blocks the entrance to a larger extent than in agGSTe2, making it difficult for substrates to access an appropriate position in the binding pocket. Therefore, slight conformational changes of these side chains would be required to accommodate substrates, not only GSH, but also other co-substrates.

Among the residues in the C-terminal domain of MdGST6B, Phe108 and Arg113 occupy the space adjacent GSH (Fig. 4B). An ionic bridge interaction and hydrogen bond network (electron-sharing network) around GSH was proposed to promote formation of anionic glutathione (GS-) in *A. dirus* GST [21]. Wang et al. [18] conjectured that Arg112 in agGSTe2, corresponding to Arg113 of MdGST6B (Fig. 3 and Fig. 4C), is involved in an electron-sharing network that stabilizes the thiolate of GSH. agGSTe2 also possesses phenylalanine at position 108, a residue believed to be part of the

Table 2
Kinetic parameters of MdGST6B.

	CDNB				GSH[a]
	k_{cat} (s^{-1})	K_m (μM)	k_{cat}/K_m (s^{-1}/μM)	Relative efficiency (%)	(s^{-1})
Wild type	11.7	6.7	1.73	100	14.0
F108G	0.99	72.8	0.014	0.81	1.13
R113A	8.0	8.4	0.95	54.9	11.0

[a] Catalytic activity toward 3 mM GSH.

putative DDT binding pocket [18], as determined from computer modeling of a DDT molecule in the pocket. To investigate the role of Phe108 and Arg113 in MdGST6B, F108G and R113A mutants were generated and assayed for their activity toward GSH and CDNB. The N-terminal His-tagged MdGST6B was used for the assay because of the possibility that mutants could lose affinity for GSH, which would make the purification process by affinity chromatography using glutathione as a ligand impossible, and for convenience in the purification procedure. The activity of MdGST6B with the N-His-tag toward CDNB (Table 2) was comparable to that of MdGST6B without the tag (k_{cat}: 25.1 s^{-1}; $K_{m:}$ 8.8 mM). The measured kinetic parameters are shown in Table 2. The affinities of wild-type and mutant MdGST6B toward GSH were too low to determine K_m and k_{cat} values precisely. Therefore, the activities of 3 mM GSH are shown in the table instead of kinetic parameters for GSH. Surprisingly, no notable changes in the kinetic parameters toward GSH and CDNB were observed when Arg113 was replaced by Ala, which suggests the hydrogen bond between Arg113 and GSH is not crucial for enzymatic activity. On the other hand, substitution of Phe108 with Gly dramatically changed the activity toward both CDNB and GSH. The K_m and k_{cat} values for CDNB were 10.9 times higher and 11.8 times lower, respectively, than those of the wild type enzyme, and the relative efficiency decreased to 0.81% in the mutant. The activity toward GSH (at a concentration of 3 mM) was 8.1% of that of the wild type. Moreover, the F108G mutant without an N-terminal His-tag failed to be retained on an affinity chromatography column using GSH as a ligand (data not shown), indicating lowered affinity toward GSH. Therefore, hydrophobic and aromatic features of Phe108 appear to be necessary for appropriate arrangement of the functional substrate binding pocket.

Helix 4 of GST is known to be distorted toward the substrate, GSH, as mentioned above (Fig. 1B) in part due to the presence of a π-helix in the middle of helix 4. In a "normal" α-helix main chain, the hydrogen atom of every backbone amino group, n, donates a hydrogen bond to the backbone carbonyl oxygen of the n−4 amino acid residue. On the other hand, a π-helix is defined by main-chain hydrogen bonds between residues five positions apart in the sequence. As shown in Fig. 4C, the π-helix segment was expanded in MdGST6B compared with agGSTe2. Since π-helices make the helical secondary structure unstable, they are considered to be located at important regions in proteins, such as active sites, through evolution [22]. This hypothesis appears to be consistent with GST where the π-helices are located just behind the bound GSH. Both epsilon-class GSTs from housefly and mosquito have two sequential phenylalanines at the same position (Phe120 and Phe121) in the sequence alignment (Fig. 3). However, their actual positions in the enzymes are not identical because of a sequence shift caused by different lengths of π-helicies in helix 4 (Fig. 4C). This difference makes the entrance to the substrate binding site of MdGST6B narrower than that of agGSTe2 (mentioned above).

For identification of structural factors that determine the substrate specificity of housefly GSTs, further analyses including site-directed mutagenesis and co-crystallization with other substrates such as CDNB and DCNB are required. In addition, information about related delta-class GSTs in *M. domestica* including MdGST1 would help to improve the current understanding of the mechanisms of substrate recognition.

References

[1] J. Hemingway, N.J. Hawkes, L. McCarroll, H. Ranson, The molecular basis of insecticide resistance in mosquitoes, Insect Biochem. Mol. Biol. 34 (2004) 653–665.

[2] D. Fournier, J.M. Bride, M. Poirie, J.B. Berge, F.W. Plapp Jr., Insect glutathione S-transferases. Biochemical characteristics of the major forms from houseflies susceptible and resistant to insecticides, J. Biol. Chem. 267 (1992) 1840–1845.

[3] A.A. Enayati, H. Ranson, J. Hemingway, Insect glutathione transferases and insecticide resistance, Insect Mol. Biol. 14 (2005) 3–8.

[4] H. Ranson, L. Rossiter, F. Ortelli, B. Jensen, X. Wang, C.W. Roth, F.H. Collins, J. Hemingway, Identification of a novel class of insect glutathione S-transferases involved in resistance to DDT in the malaria vector *Anopheles gambiae*, Biochem. J. 359 (2001) 295–304.

[5] M. Syvanen, Z.H. Zhou, J.Y. Wang, Glutathione transferase gene family from the housefly *Musca domestica*, Mol. Gen. Genet. 245 (1994) 25–31.

[6] M. Syvanen, Z. Zhou, J. Wharton, C. Goldsbury, A. Clark, Heterogeneity of the glutathione transferase genes encoding enzymes responsible for insecticide degradation in the housefly, J. Mol. Evol. 43 (1996) 236–240.

[7] S.H. Wei, A.G. Clark, M. Syvanen, Identification and cloning of a key insecticide-metabolizing glutathione S-transferase (MdGST-6A) from a hyper insecticide-resistant strain of the housefly *Musca domestica*, Insect Biochem. Mol. Biol. 31 (2001) 1145–1153.

[8] J.Y. Wang, S. McCommas, M. Syvanen, Molecular cloning of a glutathione S-transferase overproduced in an insecticide-resistant strain of the housefly (*Musca domestica*), Mol. Gen. Genet. 227 (1991) 260–266.

[9] W.H. Habig, M.J. Pabst, W.B. Jakoby, Glutathione S-transferases. The first enzymatic step in mercapturic acid formation, J. Biol. Chem. 249 (1974) 7130–7139.

[10] A.G.W. Leslie, H.R. Powell (Eds.), Processing Diffraction Data with Mosflm (2007).

[11] P. Evans, Scaling and assessment of data quality, Acta Crystallogr. D 62 (2006) 72–82.

[12] M.D. Winn, C.C. Ballard, K.D. Cowtan, E.J. Dodson, P. Emsley, P.R. Evans, R.M. Keegan, E.B. Krissinel, A.G. Leslie, A. McCoy, S.J. McNicholas, G.N. Murshudov, N.S. Pannu, E.A. Potterton, H.R. Powell, R.J. Read, A. Vagin, K.S. Wilson, Overview of the CCP4 suite and current developments, Acta Crystallogr. D 67 (2011) 235–242.

[13] A. Vagin, A. Teplyakov, MOLREP: an automated program for molecular replacement, J. Appl. Cryst. 30 (1997) 1022–1025.

[14] A.T. Brunger, P.D. Adams, G.M. Clore, W.L. DeLano, P. Gros, R.W. Grosse-Kunstleve, J.S. Jiang, J. Kuszewski, M. Nilges, N.S. Pannu, R.J. Read, L.M. Rice, T. Simonson, G.L. Warren, Crystallography & NMR system: a new software suite for macromolecular structure determination, Acta Crystallogr. D 54 (1998) 905–921.

[15] G.N. Murshudov, A.A. Vagin, E.J. Dodson, Refinement of macromolecular structures by the maximum-likelihood method, Acta Crystallogr. D 53 (1997) 240–255.

[16] J. Wongsantichon, A.J. Ketterman, An intersubunit lock-and-key 'clasp' motif in the dimer interface of Delta class glutathione transferase, Biochem. J. 394 (2006) 135–144.

[17] Y. Ding, F. Ortelli, L.C. Rossiter, J. Hemingway, H. Ranson, The *Anopheles gambiae* glutathione transferase supergene family: annotation, phylogeny and expression profiles, BMC Genomics 4 (2003) 35.

[18] Y. Wang, L. Qiu, H. Ranson, N. Lumjuan, J. Hemingway, W.N. Setzer, E.J. Meehan, L. Chen, Structure of an insect epsilon class glutathione S-transferase from the malaria vector *Anopheles gambiae* provides an explanation for the high DDT-detoxifying activity, J. Struct. Biol. 164 (2008) 228–235.

[19] L. Chen, P.R. Hall, X.E. Zhou, H. Ranson, J. Hemingway, E.J. Meehan, Structure of an insect delta-class glutathione S-transferase from a DDT-resistant strain of the malaria vector *Anopheles gambiae*, Acta Crystallogr. D 59 (2003) 2211–2217.

[20] P.G. Board, M. Coggan, M.C. Wilce, M.W. Parker, Evidence for an essential serine residue in the active site of the Theta class glutathione transferases, Biochem. J. 311 (1995) 247–250.

[21] P. Winayanuwattikun, A.J. Ketterman, An electron-sharing network involved in the catalytic mechanism is functionally conserved in different glutathione transferase classes, J. Biol. Chem. 280 (2005) 31776–31782.

[22] R.B. Cooley, D.J. Arp, P.A. Karplus, Evolutionary origin of a secondary structure: pi-helices as cryptic but widespread insertional variations of alpha-helices that enhance protein functionality, J. Mol. Biol. 404 (2010) 232–246.